

# Direct Measurements of Erythromycin's Effect on Protein Synthesis Kinetics in Living Bacterial Cells

A. Carolin Seefeldt<sup>†</sup>, Javier Aguirre Rivera<sup>†</sup> and Magnus Johansson<sup>\*</sup>

Department of Cell and Molecular Biology, Uppsala University, Sweden

Correspondence to Magnus Johansson: [m.johansson@icm.uu.se](mailto:m.johansson@icm.uu.se) (M. Johansson)

<https://doi.org/10.1016/j.jmb.2021.166942>

Edited by Ruben L. Gonzalez

## Abstract

Macrolide antibiotics, such as erythromycin, bind to the nascent peptide exit tunnel (NPET) of the bacterial ribosome and modulate protein synthesis depending on the nascent peptide sequence. Whereas *in vitro* biochemical and structural methods have been instrumental in dissecting and explaining the molecular details of macrolide-induced peptidyl-tRNA drop-off and ribosome stalling, the dynamic effects of the drugs on ongoing protein synthesis inside live bacterial cells are far less explored. In the present study, we used single-particle tracking of dye-labeled tRNAs to study the kinetics of mRNA translation in the presence of erythromycin, directly inside live *Escherichia coli* cells. In erythromycin-treated cells, we find that the dwells of elongator tRNA<sup>Phe</sup> on ribosomes extend significantly, but they occur much more seldom. In contrast, the drug barely affects the ribosome binding events of the initiator tRNA<sup>fMet</sup>. By overexpressing specific short peptides, we further find context-specific ribosome binding dynamics of tRNA<sup>Phe</sup>, underscoring the complexity of erythromycin's effect on protein synthesis in bacterial cells.

© 2021 The Author(s). Published by Elsevier Ltd. This is an open access article under the CC BY license (<http://creativecommons.org/licenses/by/4.0/>).

## Introduction

Ribosome-catalyzed protein synthesis is one of the most critical processes in any living cell. In bacteria, several different classes of antibiotics specifically target ribosomes or translation-related protein factors.<sup>1</sup> Erythromycin (ERY), of the macrolide family of antibiotics, targets mostly gram-positive and a small range of gram-negative bacteria by binding to the nascent peptide exit tunnel (NPET) (recently reviewed in<sup>2</sup>). The NPET is a cavity about 100 Å long and 10–20 Å wide, spanning through the entire large 50S ribosomal subunit. This tunnel allows the nascent peptide chain to pass through before getting released to the cytoplasm.<sup>3</sup>

Structural information on the binding site of ERY in the ribosome suggested that the drug allows translation only up to a specific peptide length, acting as a 'plug-in-the-bottle.' This hypothesis was supported by experiments showing

accumulation of peptidyl-tRNA in ERY-treated cells,<sup>4</sup> and further confirmed by additional *in vitro* experiments<sup>5,6</sup> which identified that peptidyl-tRNA drop-off occurs mostly at codon seven.<sup>5</sup> However, in further *in vitro* studies, it was also shown that peptidyl-tRNA drop-off is slow, and that, in the context of the particular experiment, a substantial fraction of the ribosomes managed to synthesize the whole 12 amino acid long peptide in the presence of the drug.<sup>7</sup> More recent cryo-EM studies of ERY-bound ribosomes show that the drug does not occupy the entire space of the tunnel but could very well allow nascent peptides to pass.<sup>8–10</sup> It is now clear that ERY treatment does not entirely inhibit translation in *E. coli* cells, as ~7% of the proteome is still produced.<sup>11</sup> More evidence that ERY modulates translation, rather than blocking it,<sup>2</sup> comes from ribosome profiling experiments, which showed that even though the highest ribosome density locates at the beginning of genes, footprints occur

throughout entire genes. In addition, these experiments also showed that ribosomes systematically stall only at particular amino acid motifs.<sup>12,13</sup>

Hence, from recent methodological advances, a new picture emerges where the mechanism of action of macrolide drugs is seemingly much more complex than the initial ‘plug-in-the-bottle’ model. *In vitro* studies,<sup>8–10,14,15</sup> and snapshots of ERY action inside the cells<sup>12,13</sup> suggest sequence-specific effects of a tunnel-bound drug, including peptidyl-tRNA drop-off, peptide by-pass (i.e., some peptides appear to be able to by-pass the bound macrolide in the tunnel), or nascent chain-mediated translational arrest. However, the questions of how all these effects combine inside the cell and what consequences they have on ongoing protein synthesis remain open.

In order to understand how ERY affects protein synthesis dynamics in the context of the living cell, we applied our recently developed single-particle tracking approach, where we follow electroporated fluorescently-labeled tRNAs inside live *E. coli* cells.<sup>16</sup> By measuring the frequency and duration of ribosome binding events of elongator [Cy5] tRNA<sup>Phe</sup> and initiator [Cy5]tRNA<sup>fMet</sup>, in the presence or absence of the drug, we observe different effects on the first codons relative to the average codon. Also, by overexpressing specific short open-reading frames, with a phenylalanine codon placed in a crucial position, we study sequence-specific dynamic effects of ERY on ongoing protein synthesis, at codon resolution in live cells.

## Results

### Severe effect of ERY on tRNA<sup>Phe</sup>-ribosome binding dynamics

The effects of ERY on translation elongation depend on the nascent peptide sequence, where three alternative scenarios have been reported:

peptidyl-tRNA drop-off,<sup>4</sup> nascent chain mediated translational arrest,<sup>17–19</sup> or peptide by-passing of the drug.<sup>11–13</sup> In order to investigate the effects of ERY on ongoing translation elongation in live cells, we used a tRNA-tracking based approach to measure the rate of translation elongation directly. We have previously shown that Cy5-labeled tRNA<sup>Phe</sup>, electroporated into *E. coli* cells, undergo repeated bindings to ribosomes.<sup>16</sup> The dwell-time of [Cy5] tRNA<sup>Phe</sup> in the slow diffusion state, i.e., ribosome-bound state, was found to be 100 ms on average. This result is in line with indirect estimates of a translation cycling time of 50 ms per codon,<sup>20,21</sup> provided that the deacylated tRNA dissociates rapidly from the ribosomal E site.<sup>22</sup>

To investigate the effect of erythromycin on the average translation elongation cycle, we electroporated [Cy5]tRNA<sup>Phe</sup> into *E. coli* cells and placed the cells on a rich-defined medium (RDM)-agarose pad under the microscope (Figure 1), as previously reported.<sup>16</sup> This time, however, after the cells had formed micro-colonies (2–16 cells), we injected a solution of RDM supplemented with 100 µg/ml erythromycin. This ERY concentration completely inhibits cell growth (Supp Figure S1). After the treatment, the cells stopped dividing and developed an elongated phenotype (Supp Figure S2). After 1 h of incubation, we acquired fluorescence movies at 639 nm laser illumination of 150–250 colonies, along with bright-field and phase-contrast images. Also, we acquired fluorescence images at 405 nm laser illumination in order to distinguish cells with a disrupted cell membrane that had taken up the dead-cell stain SYTOX blue from the agarose pad.

We analyzed the fluorescence movies using our previously reported dot detection and tracking pipeline.<sup>16,23</sup> The positions of fluorophores were detected in all frames and used to build diffusion trajectories within intact cells (i.e., not SYTOX stained), segmented based on phase-contrast

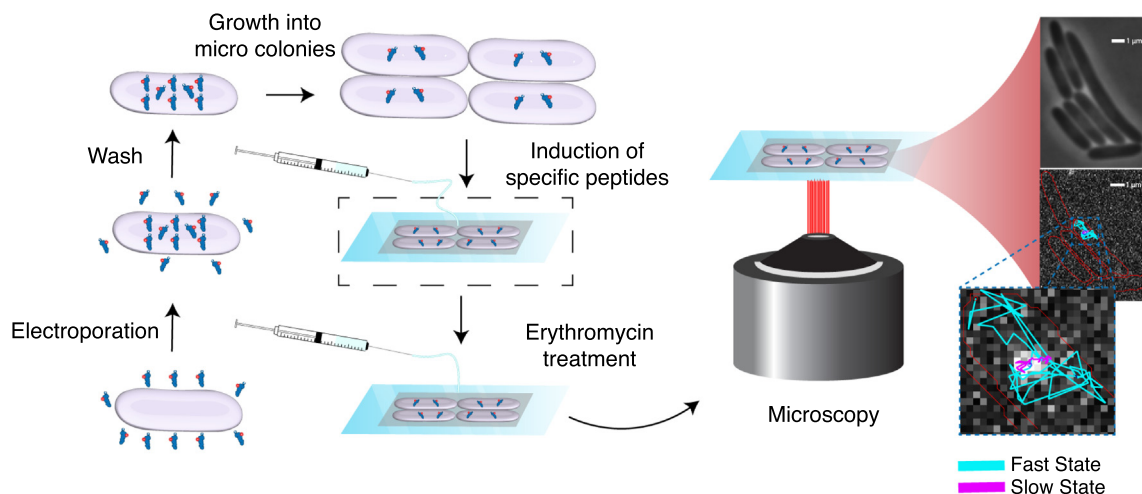


**Figure 1.** Schematic representation of the experimental method.

images. The number of trajectory steps obtained from a single experiment was between 5000 to 10,000. Based on our previous analysis of simulated microscopy data,<sup>16</sup> we know that we need more than 16,000 trajectory steps to estimate the underlying binding kinetics of the [Cy5]tRNA with reasonable precision.<sup>16</sup> Hence, we pooled the trajectories from several independent experiments for further analysis. The total number of trajectory-steps in the analysis was >25,000 for all experimental conditions.

In order to estimate the transition frequency of the labeled tRNAs between different diffusion states, we employed a Hidden-Markov-Model (HMM) based approach.<sup>16,24</sup> The model size varied from 2 to 10 discrete diffusion states. We selected the best-fit model using the Akaike Information Criterion (AIC), and further coarse-grained it to a two-state model using a threshold of  $1 \mu\text{m}^2/\text{s}$  as reported previously.<sup>16</sup> The fast state corresponds to free tRNA and tRNA bound to EF-Tu or the aminoacyl-tRNA synthetase, whereas the slow diffusion state corresponds to ribosome binding events.<sup>16</sup>

By tracking the diffusion of single [Cy5]tRNA<sup>Phe</sup> molecules inside cells, we observed that, despite treatment with a high concentration of ERY, there are clear binding events of the labeled tRNA to ribosomes (Supp Movie S1). However, from the HMM analysis, we also conclude that the average

dwell-time of [Cy5]tRNA<sup>Phe</sup> on ribosomes is prolonged significantly, from ~100 ms to ~400 ms (Figure 2(C) and Supp Table S1), in ERY-treated cells compared to untreated cells. Interestingly, the bootstrap estimate of the standard error of the dwell-time is rather high, 20% (vs. 4% in untreated cells). The larger error might suggest that, during ERY treatment, there is a much wider variation in the tRNA dwell-time on ribosomes compared to in untreated cells, perhaps due to the different peptide-sequence-dependent effects induced by the drug.

In addition to the dwell-time of the labeled tRNA on ribosomes, the HMM analysis also estimates the occupancy in the different diffusion states, i.e., the estimated steady-state fraction of tRNA<sup>Phe</sup> bound to ribosomes. When comparing the results from ERY-treated cells to data from untreated cells, we find that the slow-state occupancy decreases from 17% to 8% (Figure 2(B) and Supp Table S1). Hence, with a four-fold increase in slow-state dwell-time, but a two-fold lower slow-state occupancy, we conclude that the total average usage frequency of tRNA<sup>Phe</sup> on ribosomes inside the cells decreases by a factor of 8 during ERY treatment (Figure 2(D)).

The effect of ERY on tRNA<sup>Phe</sup> binding kinetics to ribosomes is similar to the effect caused by the antibiotic chloramphenicol (CHL), studied using

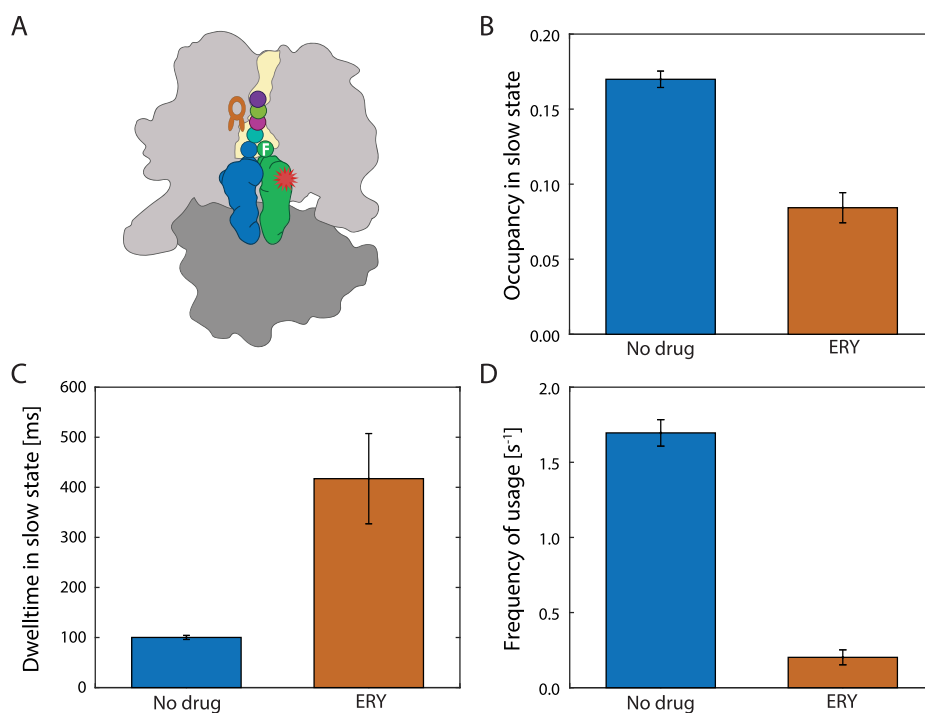


**Figure 2.** Effect of ERY on elongator [Cy5]tRNA<sup>Phe</sup> binding to the bacterial ribosome. (A) Cartoon representation of the experimental setup. Using HMM analysis, the occupancy (B) and dwell-time (C) of [Cy5]tRNA<sup>Phe</sup> bound to ribosomes were analyzed. The frequency of usage (D) was calculated from the occupancy divided by the dwell-time. Experiments were performed in the absence of ERY (blue) or 100  $\mu\text{g}/\text{ml}$  ERY (orange). Error bars represent bootstrap estimates of standard errors.

the same tRNA tracking method<sup>23</sup> – both drugs cause 3- to 4-fold longer dwell-times of [Cy5] tRNA<sup>Phe</sup> on the ribosome and 2- to 3-fold lower occupancies compared to in untreated cells. Both of these drugs target translation elongation, but in different ways. Whereas ERY allows the formation of short peptides, and in some cases even full proteins (reviewed in<sup>2</sup>), CHL has traditionally been regarded as a general elongation inhibitor, completely blocking tRNA accommodation.<sup>25,26</sup> Recent ribosome profiling results<sup>27</sup> suggest that CHL also blocks elongation in a sequence-specific manner, making it more similar to the macrolide mode of action. Nevertheless, CHL has a strong impact already during the first elongation cycle,<sup>23</sup> most likely due to its binding site at the A-site crevice. We do not, however, expect such an effect of ERY in the first elongation cycle, considering its binding site inside the nascent peptide exit tunnel.

### Unperturbed tRNA<sup>fMet</sup> usage on ribosomes in the presence of ERY

To investigate the effect of ERY on the first translation elongation cycle, we performed tRNA tracking experiments in ERY treated cells, now using Cy5-labeled initiator tRNA<sup>fMet</sup>. In this case, the dwell-time of the labeled tRNA on ribosomes reports the time required to finish translation initiation (i.e., 50S subunit joining) plus the time for the first elongation cycle.<sup>16</sup> As expected, we only see a minimal effect of ERY on the binding of [Cy5]tRNA<sup>fMet</sup> to ribosomes. Compared to in untreated cells, the dwell-time in the slow (ribosome-bound) state remains unaffected (Figure 3(C) and Supp Table S1), which is in stark contrast to the 4-fold effect on tRNA<sup>Phe</sup> bound-state dwell-time (Figure 2(C)). The occupancy of the ribosome-bound state increases slightly (Figure 3 (B) and Supp Table S1), with both numbers yielding a practically unchanged frequency of tRNA<sup>fMet</sup> usage (Figure 3(D)). Hence, in line with the current model for ERY mode of action, we find that the frequency of translation initiation, as well as the first elongation cycle, are unaffected by the drug.

### Context-specific [Cy5]tRNA<sup>Phe</sup> binding events in vivo

At the translome level, ERY treatment affects elongation strongly in an amino acid sequence-specific manner. In order to study these sequence-specific effects of ERY on translation kinetics, we constructed cell strains overexpressing short ORFs containing a phenylalanine (Phe) codon in the position where we expect to see the specific effect. We then tracked [Cy5]tRNA<sup>Phe</sup> in the presence and absence of ERY in each cell strain.

The expression of the ERY resistance methylases (*erm*), which methylate the binding site of ERY within the ribosomal tunnel, is regulated by short peptides encoded 5' of the *erm* gene. These short leader peptides act as sensors for the drug, arresting the bacterial ribosome while translating the leader peptide at a specific codon in the presence of ERY. This arrest mechanism induces the expression of a downstream *erm* gene, either by transcriptional attenuation,<sup>28</sup> or post-transcriptionally by opening up the downstream mRNA secondary structure so that a second ribosome can translate the *erm* gene.<sup>17,18</sup> The leader peptide ErmDL has been suggested to regulate the expression of ErmD post-transcriptionally.<sup>19</sup> ErmDL arrests the bacterial ribosome once codon 7 reaches the P-site. This particular Leu codon in the 7th position can be mutated to a Phe codon without abolishing the arrest.<sup>19</sup> Arrest peptides have been studied in detail using, e.g., reporter genes,<sup>29</sup> cryo-EM,<sup>8,9</sup> smFRET<sup>15</sup> and toe printing.<sup>14</sup> However, the stability of arrest peptides in the context of a living cell remains unknown.

In order to investigate the dynamics of ERY-induced translational arrest inside live cells, we overexpressed the ErmDL-L7F mRNA (Figure 4 (A)) in cells electroporated with [Cy5]tRNA<sup>Phe</sup>. We acquired fluorescence movies as described above, in peptide overexpressing cells with or without treatment with ERY. The expression of ErmDL-L7F is regulated by a T7 promoter. Hence, after induction of the T7 RNA polymerase we expect that the short-peptide mRNA constitutes the major fraction of the total mRNA in the cells.<sup>30</sup>

We observe a dramatic effect on [Cy5]tRNA<sup>Phe</sup> diffusion in ERY-treated cells overexpressing the arrest peptide with a Phe codon at the seventh position. In these cells, ERY-treatment induces a stall of nearly half of the [Cy5]tRNA<sup>Phe</sup> on ribosomes at any given moment (45% slow-state occupancy, Figure 4(B), and Supp Table S1). This occupancy can be compared to 8% slow-state occupancy in the ERY treated background strain (Figure 2(B)) or 9% occupancy in the overexpressing strain without ERY treatment (Figure 4(B)). The HMM-estimated slow-state dwell-time, 800 ms (Figure 4(C) and Supp Table S1), is also significantly longer than in the ERY-treated background strain (Figure 2(C)) or in the overexpressing strain without ERY-treatment (Figure 4(C)). However, this extended dwell-time might still be underestimated considering the frame time of data acquisition (5 ms) and a mean trajectory length of ~20 frames.<sup>16</sup> Our previous work using simulated microscopy data showed approximately 15% underestimation of a known bound-state dwell-time of 400 ms.<sup>16</sup> To investigate this scenario, we repeated the experiment at a 20 ms camera frame time. Indeed, the dwell-time of [Cy5]tRNA<sup>Phe</sup> in ERY-treated cells increased to ~7 s while the bound-state occupancy remained

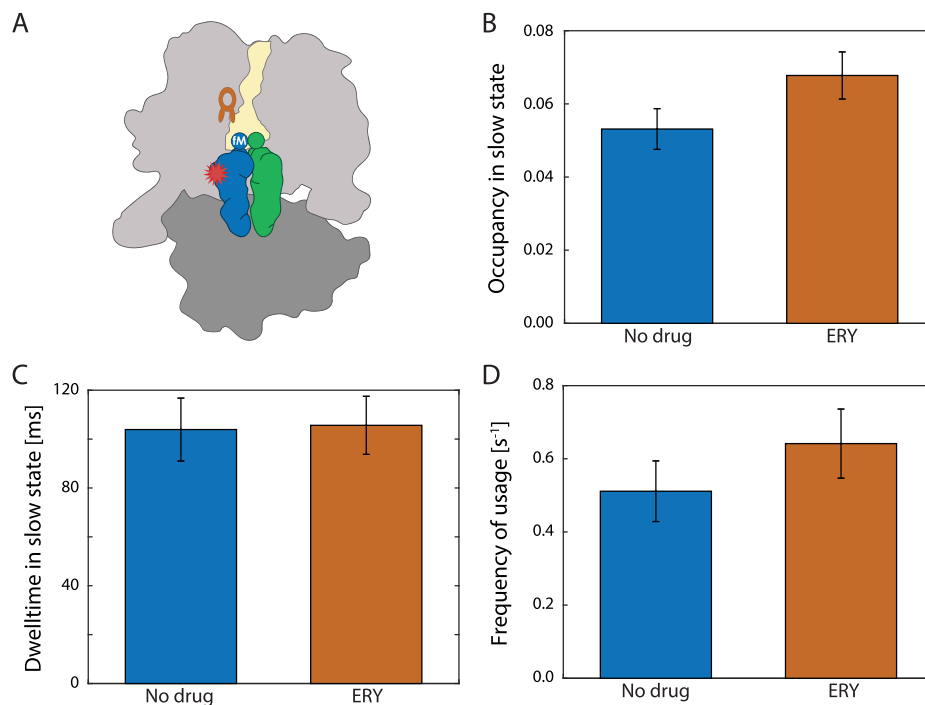


**Figure 3.** Effect of ERY on initiator [Cy5]tRNA<sup>fMet</sup> binding on the bacterial ribosome. (A) Cartoon representation of the experimental setup. Using HMM analysis, the occupancy (B) and dwell-time (C) of tRNA bound to ribosomes were analyzed. The frequency of usage (D) was calculated from the occupancy divided by the dwell-time. Experiments were performed in the absence of ERY (blue) and 100  $\mu$ g/ml ERY (orange). Error bars represent bootstrap estimates of standard errors.

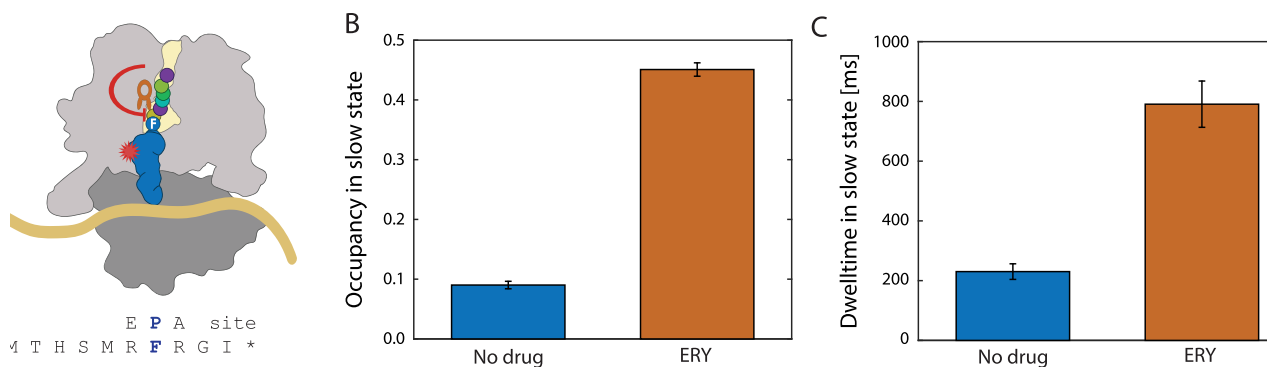


**Figure 4.** ERY arrests the bacterial ribosome on codon 7 while translating the ErmDL peptide. (A) Cartoon representation of the experimental setup. Using HMM analysis, the occupancy (B) and dwell-time (C) of [Cy5]tRNA<sup>Phe</sup> bound to ribosomes were analyzed. Experiments were performed by inducing the expression of the T7 transcribed MTHSMRFRGI\* ORF. These cells were untreated (blue) or treated with 100  $\mu$ g/ml ERY (orange). Error bars represent bootstrap estimates of standard errors.

similar to that obtained at 5 ms frame time (Supp Table S1). Our current analysis relies on tracking of both fast- and slow-diffusing tRNA. Therefore, data acquisition at longer exposure intervals becomes difficult, since the resolution of the fast state is affected. Hence, with our current experimental and analytical tools, we are limited to quantifying tRNA-ribosome binding events not longer than 1–2 seconds at a reasonable precision, and

we thus, at this point, only make the qualitative conclusion that the arrested ribosomes are stable and form long-lasting complexes in the presence of ERY.

Peptidyl-tRNA accumulates within ERY treated *E. coli* cells lacking peptidyl-tRNA hydrolase,<sup>4</sup> suggesting that ERY induces peptidyl-tRNA drop-off from the ribosome. Similar conclusions were made from studies using an *in vitro* reconstituted transla-

tion system, identifying codon 7 as the primary drop-off position.<sup>5</sup> In order to study the kinetics of peptidyl-tRNA drop-off using [Cy5]tRNA<sup>Phe</sup> tracking, we used a slightly modified version of the first 12 amino acids of the MS2 coat protein<sup>5</sup> with a Phe codon at position seven in the short ORF. The [Cy5]tRNA<sup>Phe</sup> tracking experiments were performed the same way as with the ErmDL-L7F overexpressing cells in the previous section.

Based on the HMM analysis of [Cy5]tRNA<sup>Phe</sup> trajectories in cells overexpressing the MS2CP-7F peptidyl-tRNA drop-off mRNA, we find that ERY-treatment results in longer dwell-time ( $330 \pm 60$  ms) of [Cy5]tRNA<sup>Phe</sup> on ribosomes compared to in untreated cells ( $210 \pm 20$  ms, Figure 5(C) and Supp Table S1), a significantly lower bound-state occupancy ( $8 \pm 1$  % vs.  $20 \pm 3$  %, Figure 5(B) and Supp Table S1) and frequency of usage ( $0.25 \pm 0.05$  s<sup>-1</sup> vs.  $0.95 \pm 0.15$  s<sup>-1</sup>, Figure 5(D)). However, the results are also very different from those obtained from ERY-treated cells overexpressing the ErmDL-L7F stalling ORF (Figure 4), with a much shorter bound-state dwell-time on the MS2CP-7F mRNA, and a significantly lower bound-state occupancy. Hence, the results suggest that in the presence of ERY, the ribosomes rarely reach the seventh codon of the overexpressed MS2CP-7F mRNA, and when they do, the hypothesized peptidyl-tRNA drop-off event occurs after an average ~300 ms. To corroborate

this result even further, we modified the coding region of the mRNA by moving the Phe codon to the third position, and again performed the [Cy5]tRNA<sup>Phe</sup> tracking experiment in cells overexpressing these peptides. As expected, treatment with ERY had minimal effect on [Cy5]tRNA<sup>Phe</sup> binding to ribosomes on the third codon (Figure 6).

## Discussion

Here, we present a strategy to study general as well as peptide-sequence specific effects of ERY treatment on protein synthesis in live cells. From single [Cy5]tRNA<sup>fMet</sup> and [Cy5]tRNA<sup>Phe</sup> tracking results in live *E. coli* cells, we suggest that ERY slows down the overall protein synthesis rate (Figure 2(D)) by slowing down the average elongation cycle (Figure 2(C)), while the first elongation cycle on mRNAs is barely affected (Figure 3(C)). These results are in line with previous reports showing that ERY binds in the NPET,<sup>25,26</sup> and only interfere severely with peptide bond formation after the nascent peptide has reached a certain length.<sup>5</sup>

Our finding of practically unperturbed [Cy5]tRNA<sup>fMet</sup> usage frequency in ERY-treated cells (Figure 3(D)), concurrent with significantly lower [Cy5]tRNA<sup>Phe</sup> usage frequency (Figure 2(D)),

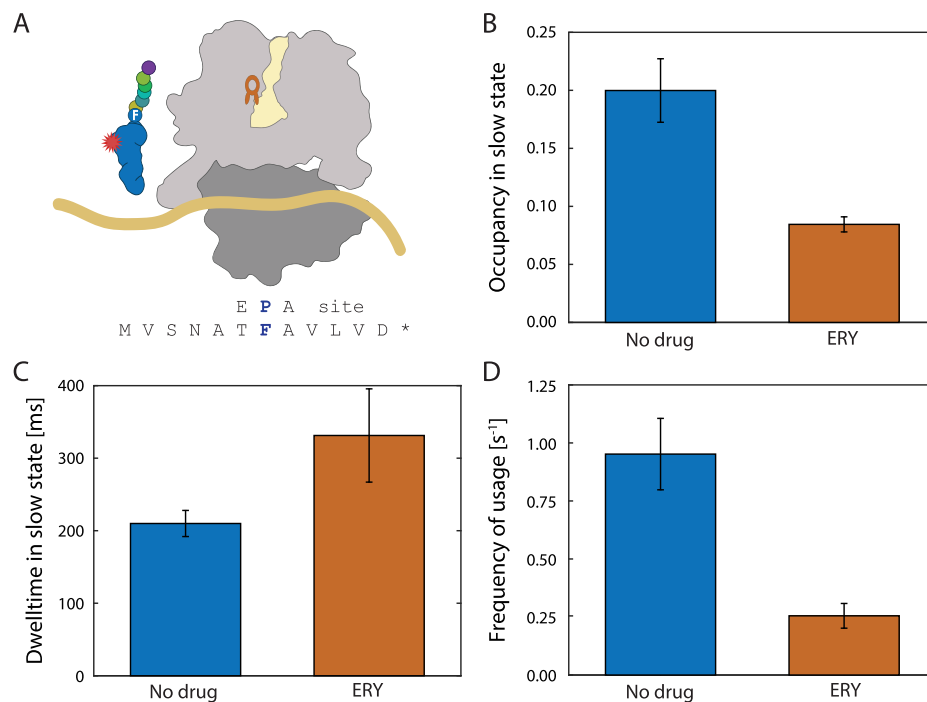


**Figure 5.** ERY induced peptidyl-tRNA drop-off from codon F7. (A) Cartoon representation of the experimental setup. Using HMM analysis, the occupancy (B) and dwell-time (C) of [Cy5]tRNA<sup>Phe</sup> bound to the ribosome was analyzed. The frequency of usage (D) was calculated from the occupancy divided by the dwell-time. Experiments were performed by inducing the T7 expressed MVSNA<sup>T</sup>FAVLVD\* ORF. These cells were untreated (blue) or treated with 100 µg/ml ERY (orange). Error bars represent bootstrap estimates of standard errors.

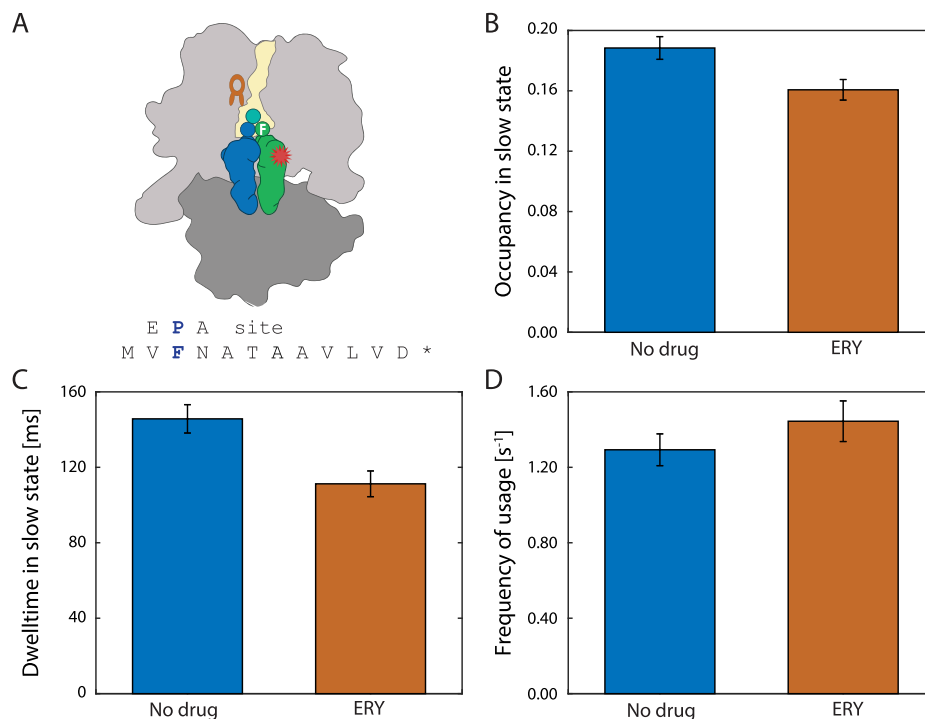


**Figure 6.** No effect of ERY on early codons. (A) Cartoon representation of the experimental setup. Using HMM analysis, the occupancy (B) and dwell-time (C) of [Cy5]tRNA<sup>Phe</sup> bound to the ribosome was analyzed. The frequency of usage (D) was calculated from the occupancy divided by the dwell-time. Experiments were performed by inducing the T7 expressed MVFNATAAVLVD\* ORF. These cells were untreated (blue) or treated with 100  $\mu$ g/ml ERY (orange). Error bars represent bootstrap estimates of standard errors.

further suggests that the number of elongation cycles per initiation event drastically decreases as a consequence of ERY binding to ribosomes. These results agree with previous ribosome profiling data showing a much higher ribosome density on earlier codons<sup>12,13</sup> and also the notion of peptidyl-tRNA drop-off as the general effect of ERY on translating ribosomes. Our results, however, suggest that ribosomes are rather quickly rescued and recycled after these prematurely terminated translation events, as we would otherwise see a much lower initiation frequency.

We further investigated, directly in live cells, the peptide-sequence specific effects induced by ERY treatment, i.e., nascent chain mediated-translational arrest, and peptidyl-tRNA drop off. In order to do so, we overexpressed mRNAs encoding short peptides known to induce the respective effect. The peptide's overexpression in the absence of the drug led to up to two-fold longer dwell-time of [Cy5]tRNA<sup>Phe</sup> on ribosomes (Figures 4(C), 5(C), and 6(C) vs. Figure 2(C)), and in one case also to lower bound-state occupancy (Figure 4(B) vs Figure 2(B)). This slight repression on translation efficiency has been seen before (Volkov 2018) and might be due to a general reduction in tRNA charging levels upon overexpressing a specific peptide sequence.

Upon ERY treatment of the peptide-overexpressing cells, the occupancy and dwell-time of [Cy5]tRNA<sup>Phe</sup> in the ribosome-bound state changed significantly when the Phe codon was inserted at the seventh position. In the case of the arrest peptide (ErmDL-L7F), the occupancy increased up to 45%, and the dwell-time increased up to several seconds (Supplemental Table 1), which is at the limit of our detection. Thus, we find that these arrested ribosomes are stable *in vivo*.

In the case of the proposed peptidyl-tRNA drop-off sequence, MS2CP-F7, our results show that the [Cy5]tRNA<sup>Phe</sup> occupancy in the ribosome-bound state decreased while the bound-state dwell-time increased in the ERY-treated cells compared to in untreated cells (Figure 5). The bound-state dwell-time of [Cy5]tRNA<sup>Phe</sup>, 300 ms is, however, considerably shorter than what would be expected from previous *in vitro* measurements of ERY-induced peptidyl-tRNA drop-off time in the order of minutes.<sup>7</sup> With our experimental setup, it is challenging to distinguish productive from unproductive [Cy5]tRNA<sup>Phe</sup> bindings to ribosomes, so the 300 ms average dwell-time detected might represent a combination of peptidyl-tRNA drop-off and productive elongation events occurring in the presence or absence of ERY in the tunnel. However,

we speculate that the dissociation of [Cy5]tRNA<sup>Phe</sup> in the MS2CP-F7-expressing cells mainly represent peptidyl-[Cy5]tRNA<sup>Phe</sup> drop-off from the ribosome, since ERY dissociation from its binding site occurs on a much longer timescale (approximately three orders of magnitude<sup>7</sup>), and since the bound-state dwell-time of [Cy5]tRNA<sup>Phe</sup> in ERY-treated cells expressing the ErmDL-L7F arrest peptide is much higher (Figures 4 and 5). If this is the case, the question of why peptidyl-tRNA drop-off is so much faster *in vivo* (hundreds of milliseconds) than *in vitro* (minutes) requires further investigation. Although the buffer composition in the *in vitro* experiments performed in reference<sup>7</sup> has been shown to yield *in vivo* compatible translation rate and accuracy,<sup>21,31</sup> there might be some additional factor present inside the cells increasing the rate of peptidyl-tRNA drop-off.

Finally, the striking difference in [Cy5]tRNA<sup>Phe</sup> usage frequency in ERY-treated cells expressing the MS2CP-F7 drop-off sequence (Figure 5(D)) compared to when the Phe codon is moved to the third position (Figure 6(D)) also suggests that few ribosomes reach codon seven during ERY treatment. This is in line with previous findings<sup>5</sup> as well as with our observation that the usage frequency of tRNA<sup>Phe</sup> is reduced significantly upon ERY treatment (Figure 2(D)) whereas the usage frequency of tRNA<sup>fMet</sup> is not (Figure 3(D)).

In conclusion, in the present study, we confirm, directly in live cells, previous *in vitro*, and indirect *in vivo* results regarding the effect of ERY-treatment on bacterial protein synthesis. In line with earlier proposals, we find that ERY does not affect the first few elongation cycles on an mRNA, whereas the average elongation cycle slows-down 4-fold. We also conclude that ERY-treatment results in a significantly higher frequency of translation initiation events relative to elongation cycles, which probably is a result of ERY-induced peptidyl-tRNA drop-off and rapid rescue of the ribosomes. Finally, based on the strikingly different results from [Cy5]tRNA<sup>Phe</sup> tracking in cell strains overexpressing either of three types of short peptides, with a Phe codon in seventh position (Figures 4 and 5) or third position (Figure 6), we can also conclude that our technique allows direct *context-dependent* measurements of translation elongation kinetics at codon resolution in live cells. Hence, we are optimistic that our method opens up for detailed measurements of mRNA-, codon-, or peptide-sequence-specific effects on translation kinetics in live cells, in the presence or absence of antibiotic drugs.

## Materials and Methods

### tRNA preparation and labeling

tRNA<sup>Phe</sup> and tRNA<sup>fMet</sup> were labeled with disulfo-Cy5 (Cy5), aminoacylated, and purified as

described before.<sup>16,23</sup> For electroporation, 1.5 pmol [Cy5]tRNA<sup>Phe</sup> or 2 pmol [Cy5]tRNA<sup>fMet</sup> were used.

### Growth experiments

The *E. coli* strain DH5 $\alpha$  was grown overnight at 37 °C in EZ rich defined media (RDM, from Teknova) supplemented with 0.2% glucose. The culture was inoculated by diluting the overnight culture 1:1000 in 300  $\mu$ l fresh RDM media supplemented with different concentrations of ERY: 0, 25, 50, or 100  $\mu$ g/ml. The growth was followed in a microplate reader (Bioscreen C, Oy) at 37 °C under aerobic conditions. Optical densities at 600 nm were measured every 5 min. Data was taken in technical replicates and analyzed with Microsoft Excel.

### Sample preparation to determine the general effect of ERY

To study the general effect of ERY on protein synthesis in live cells, 20  $\mu$ l of electroMAX DH5 $\alpha$ -*E. coli* cells (Invitrogen) supplemented with [Cy5]tRNA were transferred into a 1 mm electroporation cuvette (Molecular Bio Products) and a 1.9 kV pulse was applied using a MicroPulser (Biorad). Cells were recovered for 30 min in RDM and washed three times with fresh RDM. In the next step, cells were diluted to OD<sub>600</sub> 0.03 and placed on a 2% agarose pad containing 1  $\mu$ M SYTOX blue (Invitrogen). Cells were incubated for 100 min at 37 °C to grow into mini colonies (4–8 cells). Cells were exposed to the drug by injecting RDM supplemented with 1  $\mu$ M SYTOX blue and 100  $\mu$ g/ml ERY (or without ERY for the no-drug control). Fluorescence microscopy was performed 70–200 min after injection, or directly after the injection in the case of no-drug control. Each experiment was repeated 2–4 times.

### Sample preparation of cells overexpressing specific mRNAs

To investigate peptidyl-tRNA drop off and nascent chain mediated-translational arrest, short open reading frames of representative sequences were cloned into the pET3c vector. A T7 promoter regulated the expression of the short peptides. The sequences were designed based on previous works,<sup>5,19</sup> introducing a phenylalanine codon in the seventh position (Table 1, highlighted in bold). The sequences are listed in Table 1.

The pET3c was co-transformed with the pCS6 plasmid encoding the T7 RNA polymerase (RNAP) regulated by a pBAD promoter<sup>32</sup> into *E. coli* DH5 $\alpha$  cells. The transformed cells were made electro-competent as described in detail previously.<sup>16,23</sup> 20  $\mu$ l of the cell suspension, concentrated to OD<sub>600</sub> 60, were electroporated with 1.5 pmol [Cy5]tRNA<sup>Phe</sup> using the same settings and recovery procedure as above. Cells were

Table 1 List of cloned sequences to study erythromycin induced peptidyl-tRNA drop-off and translational arrest. The Phe codon is highlighted in bold

Expected effect	Nucleotide sequence	Amino acid sequence	Introduced mutation from the original sequence
Peptidyl-tRNA drop-off	ATG GTT TCT AAC GCT ACC <b>TTC</b> GCT GTT CTG GTT GAC TAA		MVSNATFAVLVD*
F5A, ΔQ7 Peptidyl-tRNA drop-off	ATG GTT <b>TTC</b> AAC GCT ACC GCC GCT GTT CTG GTT GAC TAA		MVFNATAAVLVD*
S3F, F5A, F7A, ΔQ7 Translational arrest	ATG ACA CAC TCA ATG AGA <b>TTT</b> CGT GGA ATC TGA	MTHSMRFRGI*	L7F

incubated for 100 min at 37 °C before induction with preheated RDM supplemented with 1 μM SYTOX blue, 0.2% (v/w) L-arabinose, and 1 mM cAMP. Induced cells were imaged 45–120 min after injection. For treatment with erythromycin, the induction media was replaced with fresh, preheated (37 °C) induction media supplemented with 100 μg/ml ERY after 45 min after the first injection. Imaging was performed 45–120 min after erythromycin injection. Each experiment was repeated 2 to 7 times.

### Optical setup

The optical setup was used as published previously.<sup>16,23</sup> For each position, bright-field, phase contrast, and fluorescence images were recorded. [Cy5]tRNA tracking was performed using a 639 nm laser (Coherent Genesis MX 639–1000 STM) set to an output density of 5 kW/cm<sup>2</sup> on the sample plane. The sample was illuminated with 1.5 ms pulses during 5 ms camera exposure. Dead cells were identified using SYTOX blue, which was assayed by illumination with a 405 nm laser using an output density of 4 W/cm<sup>2</sup> and a camera exposure of 21 ms. The microscope was operated by μManager 1.4 together with an in-house plug-in for automatic data acquisition.

### Single-particle tracking

The pipeline for data analysis has been explained in detail previously.<sup>16</sup> In summary, phase-contrast images were used to segment the cells using the published algorithm.<sup>33</sup> Dead cells, as well as partially segmented cells, were omitted from the analysis. Also, cells with none or more than two fluorophores were omitted from the analysis. The radial symmetry-based method was used for dot detection,<sup>34</sup> and dot positions were refined using a symmetric Gaussian spot model and maximum posterior fit.<sup>24</sup> Trajectories were built using uTrack,<sup>35</sup> allowing gaps of three missing points but restricting to a maximum search radius of 20 pixels in general. However, during the peptide over-expression experiments, which required a more

extended time between sample preparation (electroporation) and data acquisition, we observed a higher proportion of very fast diffusing fluorophores, maybe representing free fluorophores from degraded tRNAs. By restricting the search radius to 8 pixels, we were able to omit these fast diffusing fluorophores from the analysis. Datasets using the same tracking parameters were pooled together.

To extract the diffusional properties from the generated trajectories, we applied a Hidden Markov modeling (HMM) algorithm<sup>24</sup> to calculate tRNA's transition probability between different diffusive states. The number of diffusion states was pre-set, and the best-fit model was selected using the Akaike Information Criterion (AIC) with maximum 10 states. Since we are mainly interested in ribosome-binding events, and since the use of AIC seems to overestimate the number of discrete diffusion states,<sup>16</sup> the selected model was coarse-grained into a two-state model consisting of a “slow”, ribosome-bound state, and a “fast” state combining free tRNA and tRNA bound to the aaRS or EF-Tu. The threshold value between those states was set to 1 μm<sup>2</sup>/s, as in.<sup>16</sup> It should be noted that coarse-grained values vary only minimally with original model size, and our conclusions do not depend on any particular model size for any dataset. Dwell-times in the ribosome-bound state were calculated from the estimated state transition probabilities.<sup>16</sup>

### Author contributions

M.J. conceived the project. A.C.S. and M.J. designed the experiments. A.C.S. and J.A.R. performed experiments and analysis. All authors wrote the manuscript.

### Data availability

Microscopy data that support the findings of this study is available at the open research repository Zenodo (DOI: <https://doi.org/10.5281/zenodo.3909348>).

## DECLARATION OF COMPETING INTEREST

The authors declare that they have no known competing financial interests or personal relationships that could have appeared to influence the work reported in this paper.

## Acknowledgments

This work was supported by The Swedish Research Council (M.J. 2015-04111, 2016-06264, 2019-03714), The Wenner-Gren Foundations (A.C.S., M.J.), Consejo Nacional de Ciencia y Tecnología (CONACYT, J.A.R.), and Carl Tryggers Stiftelse för Vetenskaplig Forskning (M.J. 15:243; M.J., A.C.S. 17:226).

## Appendix A. Supplementary Data

Supplementary data to this article can be found online at <https://doi.org/10.1016/j.jmb.2021.166942>.

Received 2 September 2020;

Accepted 9 March 2021;

Available online 18 March 2021

### Keywords:

single-molecule tracking;  
mRNA translation;  
ribosome;  
macrolide antibiotics;  
tRNA

† These authors contributed equally.

## References

- Rodnina, M.V., (2016). The ribosome in action: Tuning of translational efficiency and protein folding. *Protein Sci.*, **25**, 1390–1406. <https://doi.org/10.1002/pro.2950>.
- Vázquez-Laslop, N., Mankin, A.S., (2018). How Macrolide Antibiotics Work. *Trends Biochem. Sci.*, **43**, 668–684. <https://doi.org/10.1016/J.TIBS.2018.06.011>.
- Nissen, P., Hansen, J., Ban, N., Moore, P.B., Steitz, T.A., (2000). The structural basis of ribosome activity in peptide bond synthesis. *Science (80-)*, **289**, 920–930.
- Menninger, J.R., Otto, D.P., (1982). Erythromycin, carbomycin, and spiramycin inhibit protein synthesis by stimulating the dissociation of peptidyl-tRNA from ribosomes. *Antimicrob. Agents Chemother.*, **21**, 811–818. <https://doi.org/10.1128/AAC.21.5.811>.
- Tenson, T., Lovmar, M., Ehrenberg, M., (2003). The Mechanism of Action of Macrolides, Lincosamides and Streptogramin B Reveals the Nascent Peptide Exit Path in the Ribosome. *J. Mol. Biol.*, **330**, 1005–1014. [https://doi.org/10.1016/S0022-2836\(03\)00662-4](https://doi.org/10.1016/S0022-2836(03)00662-4).
- Otaka, T., Kaji, A., (1975). Release of (oligo)peptidyl tRNA from ribosomes by erythromycin A. *Proc. Natl. Acad. Sci. USA*, **72**, 2649–2652. <https://doi.org/10.1073/pnas.72.7.2649>.
- Lovmar, M., Tenson, T., Ehrenberg, M., (2004). Kinetics of macrolide action: the josamycin and erythromycin cases. *J. Biol. Chem.*, **279**, 53506–53515. <https://doi.org/10.1074/jbc.M401625200>.
- Arenz, S., Meydan, S., Starosta, A.L., Berninghausen, O., Beckmann, R., Vázquez-Laslop, N., Wilson, D.N., (2014). Drug Sensing by the Ribosome Induces Translational Arrest via Active Site Perturbation. *Mol. Cell*, **56**, 446–452. <https://doi.org/10.1016/J.MOLCEL.2014.09.014>.
- Arenz, S., Bock, L.V., Graf, M., Innis, C.A., Beckmann, R., Grubmüller, H., Vaiana, A.C., Wilson, D.N., (2016). A combined cryo-EM and molecular dynamics approach reveals the mechanism of ErmBL-mediated translation arrest. *Nature Commun.*, **7** <https://doi.org/10.1038/ncomms12026>.
- Arenz, S., Ramu, H., Gupta, P., Berninghausen, O., Beckmann, R., Vázquez-Laslop, N., Mankin, A.S., Wilson, D.N., (2014). Molecular basis for erythromycin-dependent ribosome-stalling during translation of the ErmBL leader peptide. *Nature Commun.*, **5**, 3501. <https://doi.org/10.1038/ncomms4501>.
- Kannan, K., Vázquez-Laslop, N., Mankin, A.S., (2012). Selective Protein Synthesis by Ribosomes with a Drug-Obstructed Exit Tunnel. *Cell*, **151**, 508–520. <https://doi.org/10.1016/J.CELL.2012.09.018>.
- Kannan, K., Kanabar, P., Schryer, D., Florin, T., Oh, E., Bahroos, N., Tenson, T., Weissman, J.S., et al., (2014). The general mode of translation inhibition by macrolide antibiotics. *Proc. Natl. Acad. Sci. USA*, **111**, 15958–15963. <https://doi.org/10.1073/pnas.1417334111>.
- Davis, A.R., Gohara, D.W., Yap, M.-N.F., (2014). Sequence selectivity of macrolide-induced translational attenuation. *Proc. Natl. Acad. Sci.*, **111**, 15379–15384.
- Vázquez-Laslop, N., Thum, C., Mankin, A.S., (2008). Molecular Mechanism of Drug-Dependent Ribosome Stalling. *Mol. Cell*, **30**, 190–202. <https://doi.org/10.1016/J.MOLCEL.2008.02.026>.
- Johansson, M., Chen, J., Tsai, A., Kornberg, G., Puglisi, J. D., (2014). Sequence-dependent elongation dynamics on macrolide-bound ribosomes. *Cell Rep.*, **7**, 1534–1546. <https://doi.org/10.1016/j.celrep.2014.04.034>.
- Volkov, I.L., Lindén, M., Aguirre Rivera, J., Jeong, K.-W., Metev, M., Elf, J., Johansson, M., (2018). tRNA tracking for direct measurements of protein synthesis kinetics in live cells. *Nature Chem. Biol.*, **14**, 618–626. <https://doi.org/10.1038/s41589-018-0063-y>.
- Gryczan, T.J., Grandi, G., Hahn, J., Grandi, R., Dubnau, D., (1980). Conformational alteration of mRNA structure and the posttranscriptional regulation of erythromycin-induced drug resistance. *Nucleic Acids Res.*, **8**, 6081–6097. <https://doi.org/10.1093/nar/8.24.6081>.
- Horinouchi, S., Weisblum, B., (1980). Posttranscriptional modification of mRNA conformation: Mechanism that regulates erythromycin-induced resistance. *Proc. Natl. Acad. Sci. USA*, **77**, 7079–7083. <https://doi.org/10.1073/pnas.77.12.7079>.
- Hue, K.K., Bechhofer, D.H., (1992). Regulation of the macrolide-lincosamide-streptogramin B resistance gene ermD. *J. Bacteriol.*, **174**, 5860–5868. <https://doi.org/10.1128/JB.174.18.5860-5868.1992>.
- Liang, S.T., Xu, Y.C., Dennis, P., Bremer, H., (2000). mRNA composition and control of bacterial gene expression. *J. Bacteriol.*, **182**, 3037–3044. <https://doi.org/10.1128/JB.182.11.3037-3044.2000>.

21. Borg, A., Ehrenberg, M., (2015). Determinants of the rate of mRNA translocation in bacterial protein synthesis. *J. Mol. Biol.*, **427**, 1835–1847. <https://doi.org/10.1016/j.jmb.2014.10.027>.
22. Chen, J., Petrov, A., Tsai, A., O'Leary, S.E., Puglisi, J.D., (2013). Coordinated conformational and compositional dynamics drive ribosome translocation. *Nature Struct. Mol. Biol.*, **20**, 718–727. <https://doi.org/10.1038/nsmb.2567>.
23. Volkov, I.L., Seefeldt, A.C., Johansson, M., (2019). Tracking of single tRNAs for translation kinetics measurements in chloramphenicol treated bacteria. *Methods*, **162–163**, 23–30. <https://doi.org/10.1016/j.YMETH.2019.02.004>.
24. Lindén, M., Ćurić, V., Amselem, E., Elf, J., (2017). Pointwise error estimates in localization microscopy. *Nature Commun.*, **8**, 1–9. <https://doi.org/10.1038/ncomms15115>.
25. Bulkley, D., Innis, C.A., Blaha, G., Steitz, T.A., (2010). Revisiting the structures of several antibiotics bound to the bacterial ribosome. *Proc. Natl. Acad. Sci. USA*, **107**, 17158–17163. <https://doi.org/10.1073/pnas.1008685107>.
26. Dunkle, J.A., Xiong, L., Mankin, A.S., Cate, J.H.D., (2010). Structures of the Escherichia coli ribosome with antibiotics bound near the peptidyl transferase center explain spectra of drug action. *Proc. Natl. Acad. Sci. USA*, **107**, 17152–17157. <https://doi.org/10.1073/pnas.1007988107>.
27. Marks, J., Kannan, K., Roncase, E.J., Klepacki, D., Kefi, A., Orelle, C., Vázquez-Laslop, N., Mankin, A.S., (2016). Context-specific inhibition of translation by ribosomal antibiotics targeting the peptidyl transferase center. *Proc. Natl. Acad. Sci. USA*, **113**, 12150–12155. <https://doi.org/10.1073/pnas.1613055113>.
28. Kwak, J.H., Choi, E.C., Weisblum, B., (1991). Transcriptional attenuation control of ermK, a macrolide-lincosamide-streptogramin B resistance determinant from *Bacillus licheniformis*. *J. Bacteriol.*, **173**, 4725–4735. <https://doi.org/10.1128/jb.173.15.4725-4735.1991>.
29. Gupta, P., Kannan, K., Mankin, A.S., Vázquez-Laslop, N., (2013). Regulation of Gene Expression by Macrolide-Induced Ribosomal Frameshifting. *Mol. Cell*, **52**, 629–642. <https://doi.org/10.1016/J.MOLCEL.2013.10.013>.
30. Studier, F.W., Moffatt, B.A., (1986). Use of bacteriophage T7 RNA polymerase to direct selective high-level expression of cloned genes. *J. Mol. Biol.*, **189**, 113–130. [https://doi.org/10.1016/0022-2836\(86\)90385-2](https://doi.org/10.1016/0022-2836(86)90385-2).
31. Johansson, M., Bouakaz, E., Lovmar, M., Ehrenberg, M., (2008). The Kinetics of Ribosomal Peptidyl Transfer Revisited. *Mol. Cell*, **30**, 589–598. <https://doi.org/10.1016/j.molcel.2008.04.010>.
32. Schmidt, C.M., Shis, D.L., Nguyen-Huu, T.D., Bennett, M. R., (2012). Stable maintenance of multiple plasmids in *E. coli* using a single selective marker., *ACS. Synth. Biol.*, **1**, 445–450. <https://doi.org/10.1021/sb3000589>.
33. Ranefall, P., Sadanandan, S.K., Wahlby, C., (2016). Fast adaptive local thresholding based on ellipse fit. In: *Proc. - Int. Symp. Biomed. Imaging.*. IEEE Computer Society, pp. 205–208. <https://doi.org/10.1109/ISBI.2016.7493245>.
34. Loy, G., Zelinsky, A., (2003). Fast radial symmetry for detecting points of interest. *IEEE Trans. Pattern Anal. Mach. Intell.*, **25**, 959–973. <https://doi.org/10.1109/TPAMI.2003.1217601>.
35. Jaqaman, K., Loerke, D., Mettlen, M., Kuwata, H., Grinstein, S., Schmid, S.L., Danuser, G., (2008). Robust single-particle tracking in live-cell time-lapse sequences. *Nature Methods*, **5**, 695–702. <https://doi.org/10.1038/nmeth.1237>.